JACC: BASIC TO TRANSLATIONAL SCIENCE VOL. 8, NO. 2, 2023

STATE-OF-THE-ART REVIEW

Mechanisms of the "No-Reflow" Phenomenon After Acute Myocardial Infarction

Potential Role of Pericytes

Sanjiv Kaul, MD,[a] Carmen Methner, PhD,[a] Zhiping Cao, PhD,[a] Anusha Mishra, PhD[a,b]

HIGHLIGHTS

- **Pericytes contract during myocardial ischemia resulting in capillary constriction and no reflow.**
- **Reversing pericyte contraction pharmacologically reduces no reflow and infarct size.**
- **These findings open up an entire new venue of research aimed at pericyte function.**

SUMMARY

Pericytes contract during myocardial ischemia resulting in capillary constriction and no reflow. Reversing pericyte contraction pharmacologically reduces no reflow and infarct size. These findings open up an entire new venue of research aimed at altering pericyte function in myocardial ischemia and infarction. (J Am Coll Cardiol Basic Trans Science 2023;8:204–220)

All knowledge, like all ignorance, deviates from the truth in an opportunistic direction'
—Gunnar Myrdal[1]

There have been several reviews on the no-reflow phenomenon in recent years,[2-4] including an authoritative one by Kloner et al[2,3] who have remained active in the field for the past 45 years. The current review is selective by design and attempts to revisit some pertinent older observations on microvascular flow after reperfusion on which newer findings regarding the role of pericytes on the no-reflow phenomena might shed more light. It also questions whether pericytes may play a wider role in myocardial ischemia and infarction in addition to their role in no reflow. The review will leave many questions unanswered, which would lend themselves to future investigation.

HISTORICAL MILESTONES

The no-reflow phenomenon pertains to lack of parenchymal microvascular perfusion despite restoration of arterial blood flow after ischemia. **Table 1** lists the historical milestones related to the no-reflow phenomenon in experimental models of ischemia/infarction. Although the term "no reflow" was coined by Majno et al[5] based on findings in the

From the [a]Knight Cardiovascular Institute, Oregon Health and Science University, Portland, Oregon, USA; and the [b]Jungers Center for Neurosciences Research, Department of Neurology, School of Medicine, Oregon Health and Science University, Portland, Oregon, USA.
The authors attest they are in compliance with human studies committees and animal welfare regulations of the authors' institutions and Food and Drug Administration guidelines, including patient consent where appropriate. For more information, visit the Author Center.

Manuscript received May 20, 2022; revised manuscript received June 13, 2022, accepted June 13, 2022.

ISSN 2452-302X https://doi.org/10.1016/j.jacbts.2022.06.008

brain in 1967, the finding of sluggish tissue flow after reversal of ischemia was first described by Harman[6] in 1948. He noted slow penetration and retention of dye in skeletal muscle of rabbits 3 hours after restoration of arterial flow following 3 hours or more of ischemia. The histopathological findings included extensive tissue edema with leukocyte infiltration and dilated capillaries containing erythrocytes but no thrombi. No venous obstruction was noted.

In 1959, Sheehan and Davis[7] described "failure of reflow" after restoration of arterial blood flow to the ischemic rabbit kidney. Whereas erythrocyte stagnation within capillaries was noted immediately after reperfusion, thrombi appeared an hour later. Similar to Harman, they found the prevalence of failed reflow to increase with longer periods of ischemia, and it was seen in almost all kidneys with >3.5 hours of ischemia. In 1966, Kovacs et al[8] presented similar findings in the adrenal gland after 1 hour of ischemia.

Krug et al[9] described no reflow in the cat heart in 1966. They found infrequent no reflow after 30 minutes of coronary occlusion, but no reflow was seen in one-half the animals after 1 hour of coronary occlusion and in all animals after 2 hours of coronary occlusion. They injected acridine orange to define the risk area and light green dye to demarcate the perfused bed after reperfusion in the beating heart and then defined risk area and no reflow postmortem. In the example from their work in **Figure 1A**, the dark area containing neither acridine orange nor the green dye was defined as the region of no reflow. Immediately after reperfusion, they found interstitial and intercellular edema, and in animals lasting 1-6 hours after reperfusion, they noted capillaries packed with erythrocytes, but no thrombi (**Figure 1B**)]. Hence, apart from the duration of arterial occlusion, the time allowed for reperfusion also seemed to affect the incidence of no reflow. They also noted myocardial hemorrhages in association with ruptured capillaries. These phenomena may be related to increased capillary permeability caused by ischemia or reperfusion, or both.

In 1968, Ames et al[10] provided an in-depth analysis of brain perfusion after arterial blood flow restoration in rabbits undergoing global brain ischemia. Regions of no reflow increased in size with the duration of ischemia, but unlike the skeletal muscle, heart, adrenals, and kidney, no reflow could be seen after as early as 5 minutes of ischemia with almost the entire cerebral hemisphere affected after only 15 minutes of ischemia. Administration of heparin had no effect on the no-reflow size but perfusing the brain with blood-free solution before inducing ischemia showed complete filling of capillaries with dye. When such brains were then perfused with a red blood suspension, no reflow was again noted, indicating that only certain-sized particles (such as erythrocytes) exhibited reduced flux in the no-reflow zone.

In 1974, Kloner et al[11] described the ultrastructural changes in coronary no reflow in a large animal model. They subjected dogs to myocardial ischemia varying from 20 to 120 minutes. One-half of the myocardial biopsies showed microvascular changes, which were prominent with occlusion periods of >1 hour. In no instance was microvascular damage seen without tissue changes, and microvascular damage always lagged behind tissue damage. Some platelet remnants and areas of hemorrhage were also noted. **Figure 1C** is an example of an electron micrograph from their paper[11] in a dog with 90 minute of coronary occlusion followed by 20 minutes of reperfusion. A capillary is seen with an erythrocyte filling the entire lumen. In general these ultrastructural findings confirmed previous histopathologic observations.

Early on, several mechanisms were proposed for no reflow. For instance, in the brain, Majno et al[5] reported swollen astrocyte feet compressing the capillaries externally. External pressure from interstitial edema was also suggested as a contributing factor.[5-11] Endothelial damage and blebbing were reported in the brain by Majno et al[5] and in the heart by Kloner et al.[11] Leukocytosis is also seen with tissue damage, although leukocyte adherence occurs principally in the venules, and initial studies of no reflow did not report tissue venous obstruction.[5-10] More recently, Yemesci et al[12] showed that compared with capillaries in normal tissue, capillaries in the no-reflow zone in the brain had a beaded appearance. The narrower regions between "beads" corresponded to the

ABBREVIATIONS AND ACRONYMS

CHP = capillary hydrostatic pressure

MBF = myocardial blood flow

MCE = myocardial contrast echocardiography

NG2 = neural glial antigen-2

TABLE 1 Timeline of Historical Events Related to the No-Reflow Phenomenon in Experimental Models of Ischemia/Infarction

Year	Author(s)	Event
1948	Harman[6]	Sluggish reflow in ischemic skeletal muscle
1959	Sheehan and Davis[7]	Failure of reflow in ischemic kidney
1966	Kovacs et al[8]	Poor reperfusion in ischemic adrenal gland
1966	Krug et al[9]	Poor reflow in the ischemic heart
1967	Majno et al[5]	Used the term "no reflow" for the first time in ischemic brain
1968	Ames et al[10]	In-depth description of no reflow in the brain, including ultrastructural findings
1974	Kloner et al[11]	Ultrastructural changes related to coronary no reflow
2009	Yemesci et al[12]	Capillary constriction caused by pericytes in brain no reflow, which is inhibited by antioxidants
2017	O'Farrell et al[13]	Pericytes implicated in coronary no reflow and their relaxation by adenosine reduced no reflow in the heart

FIGURE 1 Pathognomonic Findings Related to the No-Reflow Phenomenon

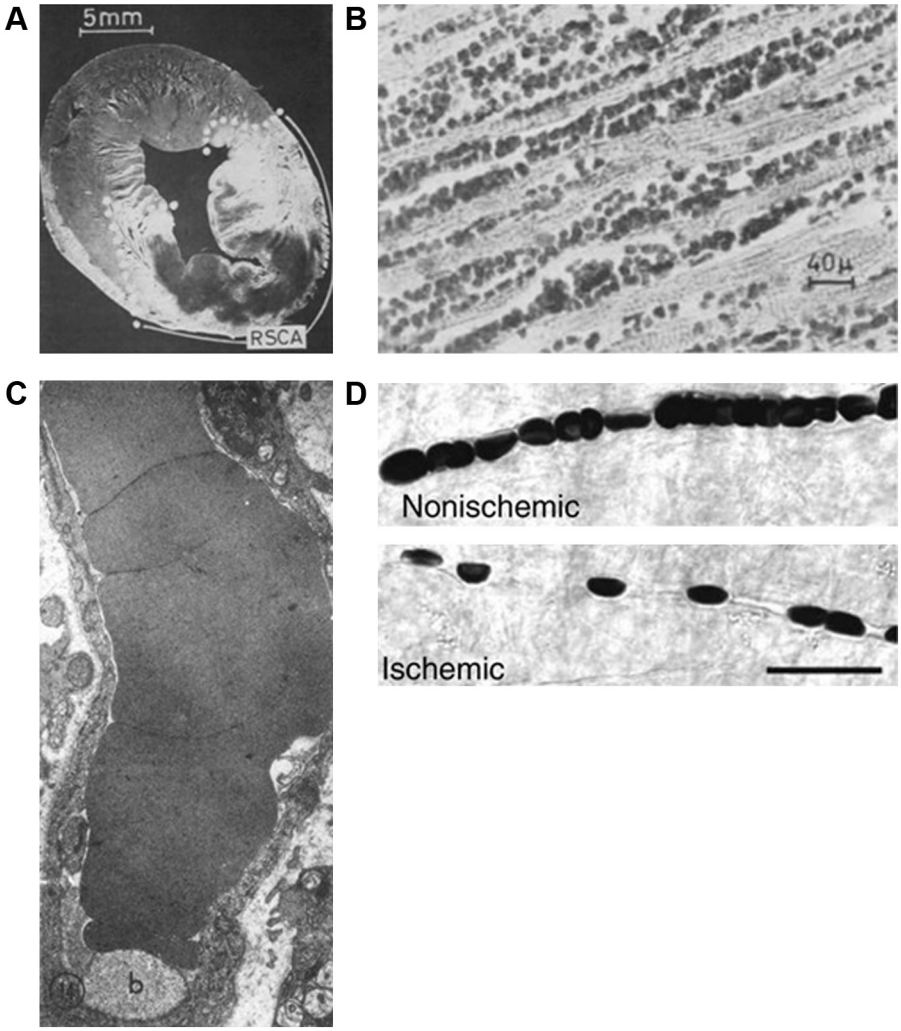

(A) An example from the first description of no reflow in the cat heart by Krug et al,[9] where they injected acridine orange in the beating heart to define the risk area and light green dye to define the perfused bed after reperfusion. Then risk area and no reflow was defined post mortem. The **dark area** with clearly demarcated borders not staining with either acridine orange or green dye denotes the no-reflow zone. This animal had undergone 2 hours of coronary occlusion followed by 3 hours of reperfusion.[9] Bar = 5 mm. Reproduced with permission of the American Heart Association. **(B)** An example of histopathologic findings in another animal in the same study by Krug et al,[9] where the heart was examined 6 hours after reperfusion following 2 hours of coronary occlusion. Myocardial capillaries are dilated, partially ruptured, and packed with erythrocytes.[9] Bar = 40 μm. Reproduced with permission of the American Heart Association. **(C)** The first ultrastructural findings in coronary reflow reported by Kloner et al[11] from a dog heart undergoing 20 minutes of coronary occlusion and 90 minutes of reperfusion. The capillary walls are thin and packed with an erythrocyte, and there is an intraluminal membrane-bound body.[11] Reproduced with permission of the American Society for Clinical Investigation. **(D)** Images taken by Yemesci et al[12] with differential inference contrast microscopy from the brain of mice undergoing ischemia and reperfusion versus sham surgery. Unlike the control mouse where capillaries appear regular, capillaries in the mice undergoing ischemia reperfusion have a beaded appearance. The narrower regions between "beads" in the experimental animal corresponds to the presence of pericytes on the abluminal surface of capillaries.[12] Bar = 20 μm. Reproduced with permission of the publisher. RSCA = region supplied by coronary artery (risk area).

presence of pericytes on the abluminal surface of capillaries. They reported that pericytes contract during ischemia and remain contracted during reperfusion. Figure 1D represents an image from their work taken with differential inference contrast microscopy.

In 2017, O'Farrell et al[13] confirmed that capillary constriction at pericyte locations was seen in

coronary no reflow in a rat model of myocardial ischemia and reperfusion. They noted that 40% of capillaries had no reflow at pericyte locations, where capillary diameter was reduced by 37%. Furthermore, they showed that adenosine increased capillary diameter by 21% at pericyte locations, decreased capillary block by 25%, and increased perfusion volume by 57%.

In the clinical setting of acute myocardial infarction, because reperfusion is mainly attempted with balloon angioplasty followed by stent placement, thrombus and/or atheroma debris are likely to be embolized to the myocardial microcirculation during the procedure.[14] Platelet activation can also occur in situ in the microcirculation under low-flow conditions.[7,15] These extraneous particles are likely to cause patchy zones of no reflow that are confined to the vascular territory of the infarct-related artery.[14,15] These patches of no reflow can, therefore, occur at the same time and within the same region as no reflow caused by prolonged ischemia and reperfusion. Clinicians have focused on reversal of these iatrogenic causes of no reflow[16-22] without appreciating that no reflow is likely to occur in infarcted regions even without manipulations of the infarct-related artery. The iatrogenic causes of no reflow and their treatment are beyond the scope of this review.

TISSUE PERFUSION IN NO REFLOW

Earlier pathologic studies using dyes to discern no reflow showed regions with clearly demarcated edges.[5-10] However, nutrient blood flow to tissue after reperfusion is complex and varies both spatially and temporally as quantified using radiolabeled microspheres and myocardial contrast echocardiography (MCE). Radiolabeled microspheres (usually 11-13 μm in diameter) used for myocardial blood flow (MBF) measurements are injected in the left atrium and lodge in small myocardial arterioles. When tissue is analyzed post mortem in a γ well counter, the amount of radioactivity in each piece of tissue can be converted to flow in $mL \cdot min^{-1} \cdot g^{-1}$.[23]

MCE uses small gas-filled microbubbles about one-half the size of erythrocytes whose microvascular rheology is identical to that of erythrocytes.[24,25] They can be detected by specially designed ultrasound equipment.[26] When injected intravenously, a majority of the microbubbles pass unhindered through the lungs and opacify the left ventricular cavity on ultrasound examination. They also enter all organs in proportion to flow to those organs and their spatial distribution on ultrasound examination reflects the spatial distribution and density of microvessels in those organs, 90% of which represent capillaries in the heart.[27] The spatial resolution of MCE is 0.5-1.0 mm depending on the ultrasound frequency used and is orders of magnitude superior to that of radiolabeled microspheres. Cardiac magnetic resonance has also provided valuable insights into the no-reflow phenomenon.[28]

In a pioneering study, Cobb et al[29] injected radiolabeled microspheres at 15 seconds, 15 minutes, 4 hours, and 3 days in separate dogs undergoing reperfusion after 2 hours of coronary occlusion. Starting from hyperemia immediately after reperfusion, they noted a progressive decline in resting MBF over time that corresponded to the extent of myocardial injury at that time. Several subsequent studies were published in the canine model of coronary ischemia and reperfusion using radiolabeled microspheres, with all showing temporal and spatial alterations in MBF within the infarct zone after reperfusion.[30-36] The greatest reduction in resting MBF after reperfusion occurred in the endocardium.[30,34,36]

Ambrosio et al[31] noted greater no reflow with longer durations of reperfusion after 90 minutes of coronary occlusion. Johnson et al[32] studied the pressure-flow relation during maximal exogenous vasodilation and found that the ischemic bed showed reduced vasodilatory reserve even after only 40 minutes of ischemia. Importantly, they noted that the decrease in coronary conductance was directly proportional to the extent of myocardial necrosis. Vanhaecke et al[33] reported similar findings and reiterated the role of exogenously administered adenosine for unmasking the reduced coronary conductance seen in reperfused tissue.

Building on these findings Villanueva et al[34] reported on MCE findings at different time points after reperfusion in dogs undergoing 3 hours of coronary occlusion. The regions showing reduced contrast enhancement at rest were generally located in the endocardium and underestimated the eventual infarct size at various intervals after reflow. But when exogenous vasodilation was used, the region with reduced contrast enhancement compared with the normal myocardium correlated very well with infarct size. **Figure 2** illustrates examples from 2 dogs with infarctions at different locations. Resting perfusion defects varied with time but with dipyridamole they corresponded to the infarct topography. Thus, all regions within the ischemic bed that ultimately underwent myocardial necrosis had reduced microvascular reserve after reperfusion.[34,35] These findings were confirmed using radiolabeled microspheres (**Figure 3A**).

FIGURE 2 In vivo Short-Axis MCE Images From Dogs During Reperfusion Following Coronary Occlusion and Infarct Size After Reperfusion

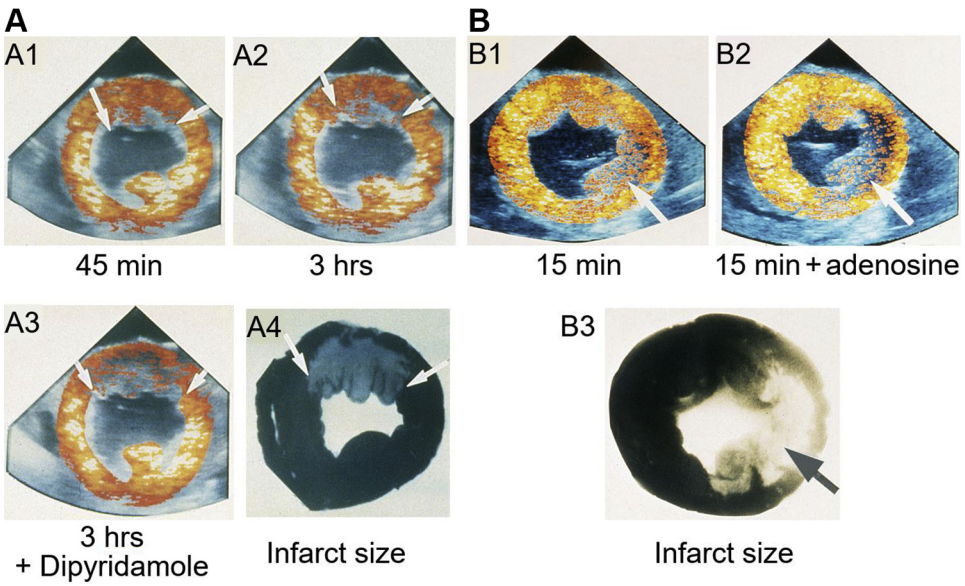

In vivo short-axis myocardial contrast echocardiographic (MCE) images from dogs during 3 hours of reperfusion following 3 hours of coronary occlusion as well as infarct size measured at 3 hours after reperfusion. **(A)** Examples from a dog with a nearly transmural anterior wall infarction involving the left anterior descending coronary artery. **(A1)** After 45 minutes of reperfusion, a small defect localized to the endocardium in the anterior wall is noted as shown by **arrows**. **(A2)** After 3 hours of reperfusion, this defect was slightly larger, as depicted by **arrows**. The addition of dipyridamole **(A3)** resulted in a much larger relative contrast defect, shown by **arrows**, which closely delineated the true size and shape of the infarct **(A4)**, indicated by **arrows**.[34] **(B)** Examples from a dog with a near transmural lateral wall infarction localized involving the left circumflex coronary artery. After 15 minutes of reperfusion, a moderate sized contrast defect is seen **(B1)** that underestimates the infarct size **(B3).** However, when adenosine is given, the perfusion defect approximates the infarct size more accurately **(B2).** Thus, the infarct size at 3 hours after reperfusion can be predicted even 15 minutes after reperfusion when adenosine is used.[36] The color maps in MCE images represent a heated object where colors change from **black to red**, to **yellow to orange** depending on degree of contrast enhancement. Reproduced with permission of the American Heart Association.

The same investigators further demonstrated that while resting MBF (measured using radiolabeled microspheres) fluctuates in the erstwhile ischemic bed over 3 hours of reperfusion, the abnormal flow reserve unmasked with adenosine remains constant over time within that bed (**Figure 3A**), starting from 15 minutes after reperfusion.[36] Thus, an MCE image taken even at 15 minutes after reperfusion during adenosine infusion will predict ultimate infarct size based on reduced microvascular flow reserve within the ischemic myocardium. They also showed that the perfusion defect size at rest correlated inversely with endocardial MBF normalized to MBF to the normal bed (**Figure 3B**).[36]

Why is MBF reserve reduced within the reperfused myocardium? The principal reason is a reduction in capillary number and/or diameter. In the absence of coronary stenosis, capillaries exert the greatest resistance to exogenously induced hyperemic flow (arterioles and venules are fully dilated).[37] The larger the number of capillaries, the greater the magnitude of hyperemic flow and vice versa. Therefore, all pathologies that result in capillary rarefaction also exhibit reduced MBF reserve.[38-40] Because resistance in a vessel is proportional to the fourth power of the radius, even a small decrease in diameter causes a large reduction in hyperemic flow. In capillaries, where erythrocytes deform to pass singly, encroachment on the capillary lumen will further slow their transit. Whenever capillary topography has been studied during reduction in coronary perfusion pressure distal to a stenosis or no reflow, in both capillary density and diameter have been reported to be reduced at pericyte locations.[41,42]

Because adenosine has been used to reduce no reflow both experimentally and clinically,[13,43,44] it is important to note that transient hyperemia caused by single venous bolus injection of a vasodilator is

FIGURE 3 Radiolabeled Microsphere–Derived Transmural MBF Data in Dogs Undergoing Coronary Occlusion Followed by Reperfusion

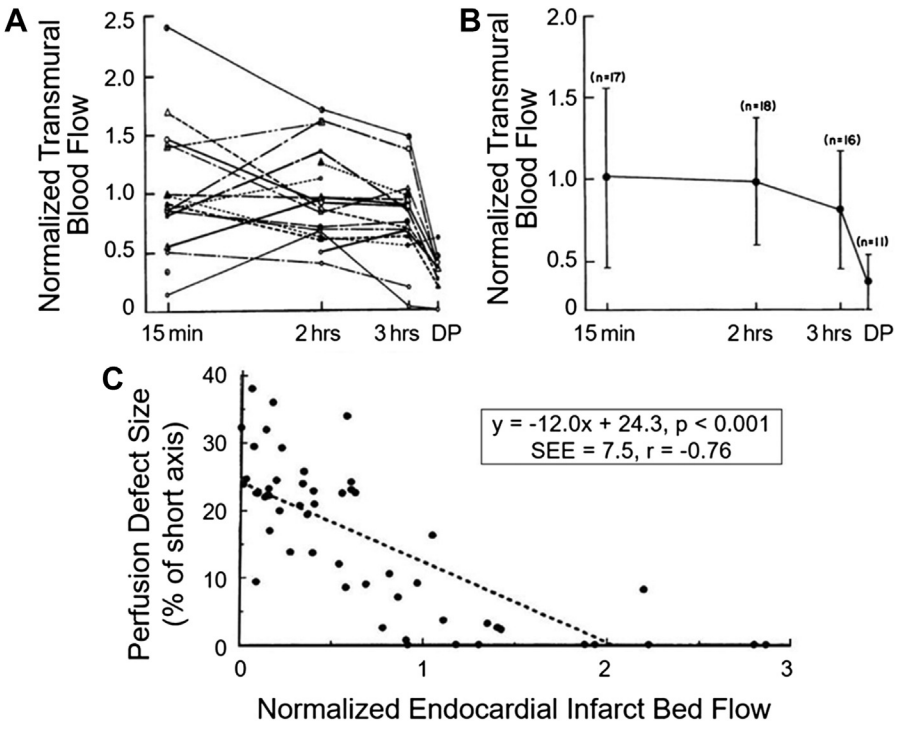

(A) Temporal changes in myocardial blood flow (MBF) from individual animals over 3 hours of coronary reperfusion.[34] MBF within the risk area is expressed as a percentage of transmural blood flow in the normal myocardium on the y-axis, and the interval after reperfusion is depicted on the x-axis. DP indicates measurements made during the infusion of dipyridamole after 3 hours of reflow. Marked temporal heterogeneity in resting MBF is noted in individual animals, with **(B)** temporal changes in the mean transmural MBF from all dogs. On average, the resting MBF in the risk area is similar to that of the normal bed and starts declining only at 3 hours after reperfusion. When DP is administered, infarcted regions show markedly reduced MBF reserve compared with the MBF reserve of the normal bed. It is during DP infusion that the spatial extent of perfusion defect on MCE reflects infarct size. **(C)** Relation between MCE defect size as a percentage of the short-axis slice (y-axis) and resting normalized endocardial blood flow within the infarct bed (x-axis) from another set of dogs.[36] These results demonstrate that MCE defect size at rest, which is located mostly in the endocardium, is determined by the level of endocardial MBF within the infarct zone. SEE = standard error of estimate.

unlikely to reduce no reflow. All it does is unmask the region of reduced microvascular reserve that will undergo necrosis if flow is not restored. When vasodilators are used pharmacologically to inhibit pericyte contraction they have to be used for a longer duration.[13,43,44]

IS NO REFLOW JUST ANOTHER MANIFESTATION OF REPERFUSION INJURY?

With few exceptions, greater emphasis has been placed on the duration of ischemia rather than the time course of reperfusion as affecting the size of the no-reflow zone. It is possible, however, that ischemia of longer duration results in more severe reperfusion injury and all the pathologic findings of no reflow are manifestations of reperfusion injury. It has also been argued that mitigating reperfusion injury might simply delay it and that reperfusion injury should be measured much later than a few hours after reperfusion. Also some have used reperfusion injury and no reflow synonymously, which is a mistake because one is predominantly a myocyte phenomenon and the other a microvascular one, even if they may be related in some instances.

A few studies using pharmacologic and nonpharmacologic interventions support the notion that no reflow is a microvascular manifestation of reperfusion injury. For example, Przyklenk and Kloner[45] showed that whereas administering superoxide dismutase and catalase just prior to reperfusion had no effect on infarct size, it markedly reduced the no-reflow zone and improved MBF in the ischemic bed. Hale et al[46] also reported a diminution in no reflow

without reduction in infarct size when moderate hypothermia was initiated in rabbits undergoing 30 minutes of ischemia followed by reperfusion. They found that hypothermia at time of reperfusion had the best effect but it also offered substantial benefit when initiated 30 minutes later. They speculated that hypothermia might reduce reperfusion injury by modulating release of oxygen free radicals. They did not measure MBF in that study. Similarly, drugs that have been used clinically to reduce no reflow (eg, adenosine, nicorandil, verapamil)[43,44,47-51] have also been shown in animal models to reduce reperfusion injury.[52-54]

If the extents of no reflow and necrosis are both related to reperfusion injury, attempts at reducing one should also reduce the other. This has been shown with several drugs, including 4-clorodiazepam, a mitochondrial membrane transporter protein agonist;[55] adiponectin, where it also improved vascular function (in diabetic rodents);[56] pitavastatin, which has anti-inflammatory properties and activates the PI3K-Akt/mTor pathway (in a porcine model);[57] dabigatran that has anti-inflammatory and anti-oxidative properties (rabbit model);[58] and, prolame, which activates signaling downstream of the estrogen receptor and enhances endothelial functions (rat model).[59]

There are some studies, however, where reduction in infarct size did not translate to diminution in the no-reflow zone. For example, Hale et al[60] showed that ranolazine reduced infarct size without affecting no reflow or ischemic MBF in a rabbit model. The same group also reported that the mitochondrial targeted drug SB-20 reduced infarct size but not no reflow.[61] They did not measure MBF in that study. Finally, Skyschally et al[62] showed reduction in infarct size but not no reflow and found no effect on regional MBF by either direct or remote preconditioning. It appears that all 3 studies showed beneficial effects of the intervention on myocyte viability without affected MBF. We have reported that intravenous ranolazine increases plasma adenosine levels by binding to cytosolic-5′nucleotidase.[63] Adenosine can provide cardioprotection independent of its effect on MBF[64] that might explain the reduction in infarct size without an effect on MBF, which would have been required to ameliorate no reflow.

ROLE OF PERICYTES IN NO REFLOW

What causes the capillary number/diameter to decrease? Our hypothesis is that when coronary autoregulation is exhausted and arteriolar dilatation can no longer control capillary hydrostatic pressure (CHP) as occurs during ischemia, pericytes contract to maintain a constant CHP.[37,41,42,65,66] Yemesci et al[12] observed pericyte contraction immediately after ischemia was produced in the brain by arterial ligation. We have observed capillary constriction at the site of pericyte location when pressure distal to a stenosis is reduced by exogenous hyperemia.[42,66]

CHP is one of the 4 forces responsible for tissue fluid hemostasis that Starling[67] described 125 years ago, the others being interstitial hydrostatic pressure as well as capillary and interstitial oncotic pressures. Within the autoregulatory range, coronary arterioles either dilate or constrict to maintain a constant CHP. When autoregulation is exhausted and blood flow becomes pressure-dependent, then, in the absence of any other control mechanism, CHP will be driven by systemic pressure, which is not conducive to cell health. Based on studies using MCE, we have shown that capillary volume decreases both when perfusion pressure falls below or rises above the autoregulatory range.[37,65] When perfusion pressure falls, such as in myocardial ischemia, we have shown that capillaries constrict at pericyte locations.[41,42] When perfusion pressure rises above the autoregulatory range, we found that capillary volume decreases and blood is shunted away from the capillary beds through arteriovenous shunts that are not active during normal conditions.[65] Pericytes can act as precapillary sphincters to close off entire capillary beds, thus producing capillary rarefaction, which can lead to heart failure.[68,69] **Figure 4** is a schematic of proposed pericyte functions for controlling tissue fluid homeostasis.

Figure 5A depicts a cartoon of pericyte location on capillaries.[66] **Figure 5B** shows their relation with capillaries in the cardiac and skeletal muscles using 2-photon microscopy.[41,42,66] These images were obtained from neural glial antigen-2 (NG2)-dsRed transgenic mice in which pericytes express the red fluorescent protein dsRed under the NG2 promoter and vessels were labeled by intravascular administration of isolectin B4 (in green) to label the vascular basement membrane. **Figure 5C** illustrates pericytes surrounding a transversely sectioned capillary on electron microscopy, and **Figure 5D** shows scanning electron microscopic images of pericytes and their primary and secondary processes encasing and impinging on capillaries from a pit viper.[70] Similar images have been obtained from the rat myocardium.[71]

Our knowledge (or ignorance) of the role of myocardial pericytes, the second most abundant type of cells in the heart,[72] is at the same stage today as our knowledge (or ignorance) was regarding the

FIGURE 4 Schematic to Depict the Potential Role of Pericytes in Tissue Fluid Hemostasis

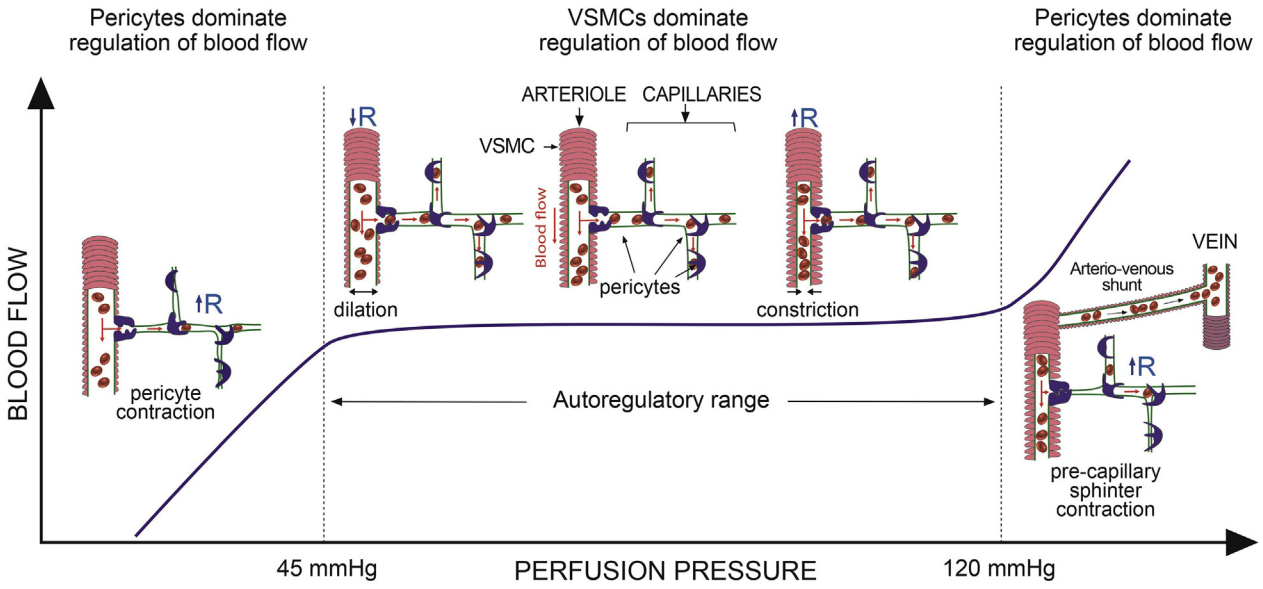

When the mean coronary perfusion pressure (CPP) ranges within the autoregulatory range, between approximately 45 mm Hg and 120 mm Hg, the vascular smooth muscle cells (VSMCs) on the resistance arterioles contract or relax to maintain a constant capillary hydrostatic pressure (CHP). When CPP falls below 45 mm Hg, the arterioles are fully dilated and cannot dilate anymore. When CPP is above 120 mm Hg, they are fully constricted and cannot constrict anymore. At CPP <45 mm Hg, pericyte contraction causes capillary constriction in order to maintain a constant CHP. At CPP >120, precapillary sphincters contract to preserve CHP and this diverts flow through arteriovenous shunts that are not operative under normal conditions. Contraction of precapillary sphincters shuts of capillary beds, thus causing capillary rarefaction, which could lead to myocardial ischemia and heart failure.[37,42,66,82] R = resistance.

endothelium 45 years ago when Furchgott showed that it was a metabolically active organ. Whereas Rouget[73] first described pericytes 150 years ago, they were overlooked for a large part of the 20th century, in part, because they were difficult to differentiate morphologically from vascular smooth muscle cells. Better phenotyping techniques, including their expression of PDGFRβ and of the proteoglycan NG2, have facilitated greater research on pericytes,[74] particularly in the eye[75] and brain,[76] including their contribution to vascular structure and permeability, blood flow regulation, immune function and wound healing, progenitor capacity, and maintenance of the blood-brain barrier.[77] Published reports are now also accumulating regarding the role of pericytes in the heart, particularly in ischemia and infarction using similar techniques to those used for the brain and eye.[78]

It is not clear how pericytes constrict capillaries. Most in vivo studies on pericyte contraction measure change in capillary dimensions at pericyte locations. Thus, their assessment of pericyte contraction is indirect because the in vivo microscopic techniques used do not have the resolution to measure pericyte dimensions. Higher resolution in vitro studies have shown that pericyte bodies get smaller rather than larger on stimulation[79] and cramp the matrix on which they are placed.[80] Simulation studies suggest that change in pericyte body shape itself can buckle the underlying capillary basement membrane and alter capillary size.[81] How pericyte processes participate in changes in capillary dimensions is not clear. Tips of the processes could elongate to dig into the abluminal capillary surface, thus creating luminal indentations (**Figure 5D**). This elongation would again lead to the processes becoming thinner rather than thicker. Using postmortem electron microscopy, we recently showed that pericytes and their processes appear thinner during myocardial ischemia than pericytes from ischemic tissue treated with adenosine do.[82]

As stated earlier, because resistance in the capillary is related to the fourth power of the radius, a very slight, even imperceptible, change in capillary dimension would make a large change in its resistance, which would increase further by impinging on erythrocyte flux. If a number of pericyte processes interact with a single capillary, resistance in the

FIGURE 5 Anatomy and Topography of Pericytes

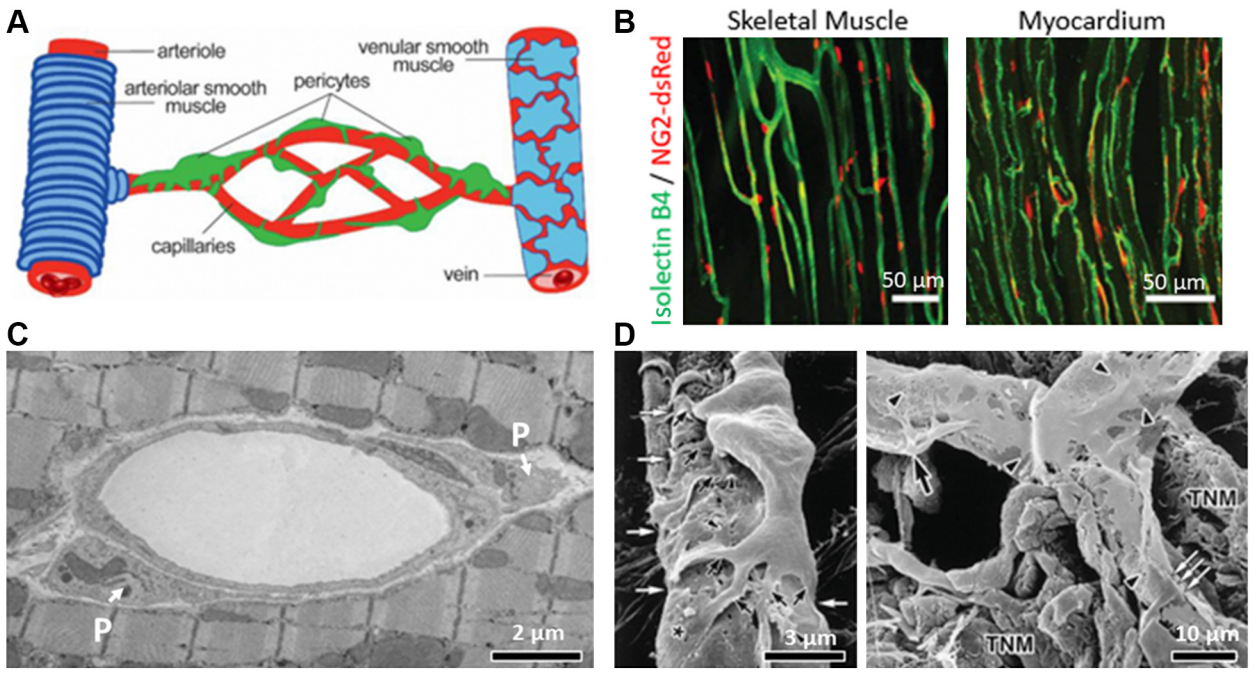

(A) Schematic of the vasculature showing arteriole **(left)** ensheathed by arteriolar smooth muscle cells **(blue),** the capillary network **(center)** enwrapped by pericytes **(green)** of different morphologies,[74] and the draining venule covered by a thin, sparse layer of smooth muscle cells **(right). (B)** Images of the microvascular network in a skeletal muscle **(left)**[42] and cardiac tissue **(right).** These images were obtained from neural glial antigen-2 (NG2)-dsRed transgenic mice in which pericytes express the red fluorescent protein dsRed under the NG2 promoter and vessels were labeled by intravascular administration of isolectin B4 **(green)** to label the vascular basement membrane. Bars = 50 μm. **(C)** Electron microscope image of capillary sectioned obliquely showing pericytes (P) at polar ends. Bar = 2 μm. **(D)** Scanning electron micrographs of capillary pericytes from a pit viper.[70] **(Left)** A pericyte extends many primary processes **(black arrows)** tightly enwrapping the endothelial tube. The **asterisk** shows a flattened secondary process. In addition, many small projections extend from the margins of the primary and secondary processes **(arrowheads).** The primary processes are seen to compress the endothelium **(white arrows).** Bar = 3 μm. **(Right)** Distribution of the secondary processes and the small projections of pericytes. **Black arrows** indicate cell bodies of pericytes, and **arrowheads** indicate the small projections. Secondary flattened processes are distributed on the capillary wall. A pericyte primary process clearly impinges on the endothelium **(white arrows).** Bar = 10 μm. It is easy to see why even a small change in shape of pericyte body or processes at 1 or multiple sites could alter capillary dimension and resistance. TNM = terminal nerve mass. Reproduced with permission of SPIE.

capillary could be altered significantly. From a design perspective, pericytes and their processes are placed at the right locations to alter resistance in the capillary network.

What does pericyte constriction of capillaries do to MBF in the ischemic zone? That the reduced MBF reserve within the ischemic bed is constant over several hours suggests that the reduction in net capillary size and or number is also constant over this time, although individual capillary beds may open or close, resulting in dynamic alterations in resting MBF.[29-36] It is unlikely that this stable coronary microvascular conductance with vasodilation is caused by events being driven primarily within the capillaries, such as endothelial swelling, erythrocyte entrapment, and so on, because these would only worsen over time. It is more likely that reduction in capillary diameter and number results from dynamic extracapillary forces that are trying to maintain a constant resistance in the capillary bed, and hence, CHP, within the ischemic myocardium. After a few hours, pericytes may start dying as either the ischemia or the reperfusion periods are extended, resulting in irreversible reduction in capillary diameter and number within the center of the infarct zone causing progressive drop in resting endocardial MBF over hours.[29,30] Because energy consumption of myocytes is higher than that of supporting cells, it may also be that myocytes die before pericytes. Evidence is accumulating, however, that pericytes in the infarcted myocardium may change phenotype to become other cells with longer ischemic durations.[78,83]

Pericytes are activated by ischemia itself independent of CHP. For instance, oxygen-glucose deprivation of cultured brain pericytes not subjected to any

FIGURE 6 **No Reflow Size Is Reduced With a Specific GPR39 Inhibitor**

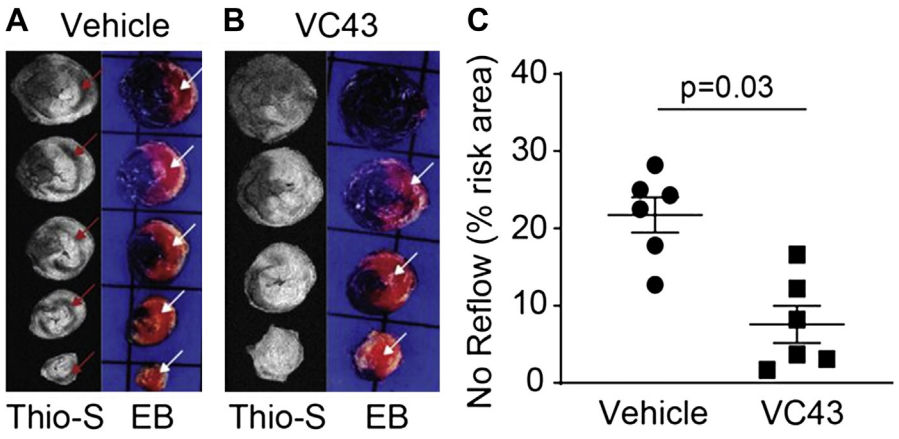

No reflow areas are the **black** areas not stained with Thioflavin-S (Thio-S) **(red arrows)** and risk areas are the zones not stained blue with Evans blue (EB) **(white arrows)** in cross-sections of the heart in wild-type mice treated with vehicle **(A)** or a specific GPR39 inhibitor, VC43 **(B).** Extensive no reflow is visible in the former and none in the latter. Aggregate data **(C)** show a 2.9-fold smaller no-reflow/risk area ratio in the VC43- versus vehicle-treated animals.[41]

hemodynamic factors reduces cell mobility within an hour and later results in apoptosis.[84] An in vivo study of retinal pericytes demonstrated that ischemia induces α-smooth muscle actin and calcium-mediated persistent pericyte contraction, which can be delayed by glucose supplied from perimicrovascular glycogen.[85] Live imaging of brain slices during simulated ischemia demonstrates that capillaries constrict at pericyte locations first and then by 40 minutes the pericytes die.[77]

Oxygen free radicals released during reperfusion can also activate pericytes. For example, Yemesci et al[12] showed capillary constriction at pericyte locations in vivo in the brain by local injection of peroxynitrite, an oxygen free radical. They were also able to attenuate capillary constriction in vivo with the nitric oxide synthase inhibitor, *N*ώ-nitro-L-arginine, as well as the superoxide scavenger *N*-tertbutyL-α-phenylnitrone administered immediately prior to reperfusion.[12] Complement released during reperfusion injury also activates pericytes that leads to their transition to fibroblasts that further impinge on the capillary lumen.[83] None of these mechanisms need be exclusive. For instance, immediate pericyte contraction may result from perturbations in microvascular hemodynamics and then be sustained by oxygen deprivation during ongoing ischemia followed by reperfusion injury, which in turn could be exacerbated by pericyte contraction itself.

Pericytes have a large number of ion channels and receptors that could be manipulated to prevent or reduce their contraction.[86] For example, adenosine can relax pericytes by activating adenosine triphosphate-sensitive K^+ channels,[87,88] and O'Farrell et al[13] reported less capillary constriction and reduced no reflow after adenosine treatment. Obviously, adenosine released during ischemia itself is not enough to prevent pericyte contraction. Clinical trials in coronary reflow have also shown benefit of adenosine.[43,44] Similarly, nicorandil has been demonstrated to reduce no reflow in the clinical setting.[48,49] It possesses the dual properties of a nitrate and adenosine triphosphate-sensitive K+ channel agonist.[89] Additionally, calcium channel blockers, such as verapamil, which have been used successfully clinically for reducing no reflow,[50,51] may reduce pericyte contraction by inhibiting L-type voltage dependent calcium channels.[90]

More recently, we reported that the orphan G-protein coupled receptor GPR39, a member of the Ghrelin receptor subfamily, is present in vascular smooth muscle cells and contributes to coronary arteriolar tone in mice.[91] We also demonstrated that activation of GPR39 by its naturally occurring ligand 15-hydroxyeicosatetraenoic acid that is released during ischemia, causes calcium release in pericytes.[41] GPR39 knockout mice and mice treated with VC43, a tool compound that is a specific GPR39 inhibitor, given 15 minutes into 1 hour of coronary occlusion showed markedly smaller no-reflow zone and infarct size 2 hours after reperfusion. These beneficial effects of the drug were associated with less capillary

FIGURE 7 Infract Size Is Reduced With a Specific GPR39 Inhibitor

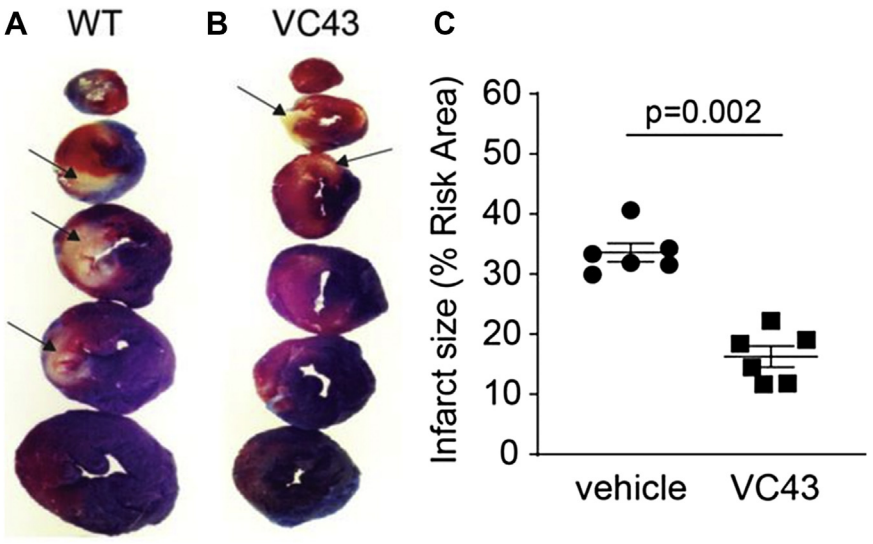

Infarct size data from wild-type (WT) mice each treated with either VC43 or vehicle. A large infarct (pale tissue marked by **black arrows**) in a vehicle-treated animal **(A)** whose risk area (tissue not stained with Evans blue dye) is similar in size to a VC43-treated animal **(B)**; the infarct size in the latter is markedly smaller. Aggregate data **(C)** show a 2-fold difference in the infarct size/risk area ratio in the VC43- versus vehicle-treated animals.[41]

constriction at pericyte locations as well as a greater capillary density.[41] **Figures 6 to 8** show results on no-reflow size, infarct size, and capillary topography in wild-type mice treated with VC43 when compared to vehicle. Inhibition of other receptors and ion channels present on pericytes that contribute to their contraction either alone or in combination, could further relax pericytes during ischemia and reperfusion, thus further reducing no reflow.

COULD PERICYTES ALSO INFLUENCE INFARCT SIZE?

It is clear that pericytes contract during ischemia because CHP needs to be maintained at as normal a level as possible. It could also result from lack of oxygen and/or glucose as well as release of metabolites that cause an increase in intracellular calcium within pericytes. It is well established that when a coronary artery is occluded, myocardial necrosis starts in the endocardium and over time extends into noncollateral-supplied regions of the risk area.[92-94] The initial endocardial injury during ischemia has been explained by reduced endocardial MBF compared to the mid- and epicardial regions of the heart. Furthermore, the reduction in endocardial MBF has been attributed to greater endocardial wall stress because the endocardium abuts the left ventricular cavity where pressures are higher than at the epicardium. Additionally capillary density has been shown to be lower in the endocardium than the epicardium both in the rat[95] as well as the human[96] heart, which likely makes the endocardium more vulnerable to ischemia.

An additional possibility may be that endocardial MBF is reduced disproportionately during ischemia from greater pericyte-mediated constriction of capillaries in the endocardium. While we have been successful at measuring MBF and regional myocardial function with good resolution, there are no reliable techniques available to measure even distal arteriolar pressures let alone CHP in a beating heart. Therefore, we cannot measure transmural vascular pressure gradients in the heart. Because flow is determined by pressure gradients, arteriolar pressure in the endocardium has to be lower than that in the epicardium under normal conditions.

When CHP falls in the presence of ischemia or reduced perfusion pressure, pericytes will contract,[12,13,37,41,42] and it is likely they will contract the most in the endocardium where CHP is likely to suffer the greatest decline. Thus, there may be a transmural gradient in the magnitude of pericyte contraction that may also lead to greater reduction in

FIGURE 8 **Capillary Density and Diameter Are Larger During Myocardial Ischemia With a Specific GPR39 Inhibitor**

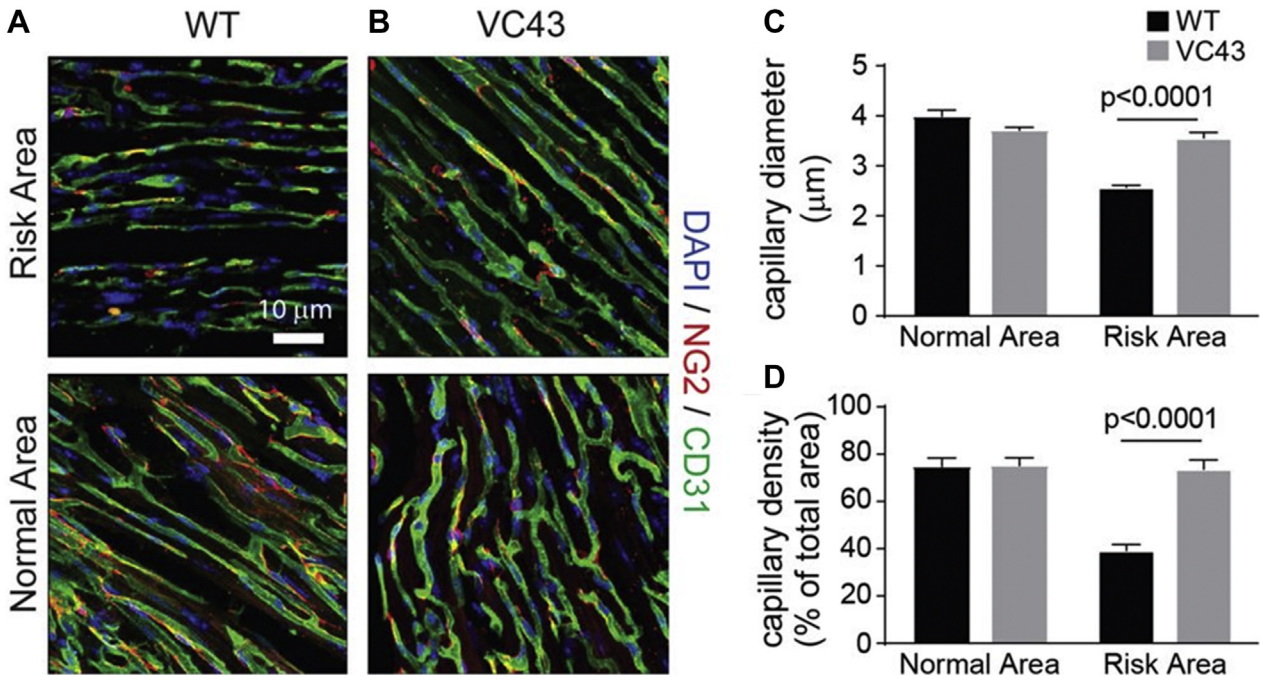

Capillary topography and pericyte locations in a WT vehicle-treated mouse **(A)** and a WT VC43-treated mouse **(B)** from within the risk area **(top)** and the normal myocardium **(bottom).** Bar = 10 μm. Capillaries are stained **green** with CD31 and pericytes are stained **red** with NG2. Both capillary size and density appear similar within the normal myocardium in both mice but appear more diminished in the risk area in the vehicle- versus the VC43-treated mouse. Quantitative analysis reveals the average capillary diameter **(C)** to be smaller in the risk area of the vehicle-treated mice compared to the VC43-treated mice, while being similar in the normal myocardium in the 2 groups of animals. Similarly, the capillary density measured as a percentage of capillaries occupying the total myocardial area viewed under the microscope **(D)** was less in the risk area of the vehicle- versus the VC43-treated mice. Capillary density was similar in the normal, nonischemic myocardium in the 2 groups of animals.[41] DAPI = 4′,6-diamidino-2-phenylindole; other abbreviations as in Figures 5 and 7.

endocardial MBF. This may explain why no reflow is more likely to be seen in the endocardium. It can also explain why VC43 that inhibits pericyte contraction not only results in less no reflow but also less necrosis. Similar results were obtained in GPR39 knockout mice.[41]

It has been known for a while that when resting perfusion pressure drops vasomotor tone is still present despite ongoing ischemia that can be unmasked with use of a coronary vasodilator such as adenosine.[97-100] It is clear that this increased tone occurs at the capillary level because capillary volume as measured by MCE decreases.[37,66] Although several mechanisms have been suggested for this finding, it is possible that pericyte contraction in response to reduced perfusion pressure might constrict capillaries and contribute to the vasomotor tone.[82] Thus, pericytes, acting as sentinels that guard tissue fluid hemostasis, may be playing a larger role in myocardial ischemia and infarction than previously was realized. Teleologically, tissue fluid hemostasis should take precedence over tissue oxygenation.[66] The mechanisms whereby changes in CHP are detected and the location where they are detected (endothelium or pericyte) are yet unknown. Preliminary results implicate the transient receptor potential ion channel subfamily M.

With prolonged ischemia, sustained reduction in CHP and/or ischemia in mid- and epicardial layers will activate pericytes there as well, ultimately leading to necrosis in those regions. Timely relief of ischemia will reverse reduction in CHP and pericyte contraction and consequently preserve the myocardium. The longer the ischemia, the more likely that pericytes will contract irreversibly and not respond even if coronary hemodynamics are restored. If pericytes play a role in the pathogenesis of myocardial ischemia and infarction, newer drugs could be developed to inhibit their contraction.

The MCE images depicted in Figure 9 are from a dog undergoing coronary occlusion for 6 hours at which time infarct size was measured without any

FIGURE 9 Spatial Extent of Perfusion During Coronary Occlusion Predicts Infarct Size 6 Hours Later

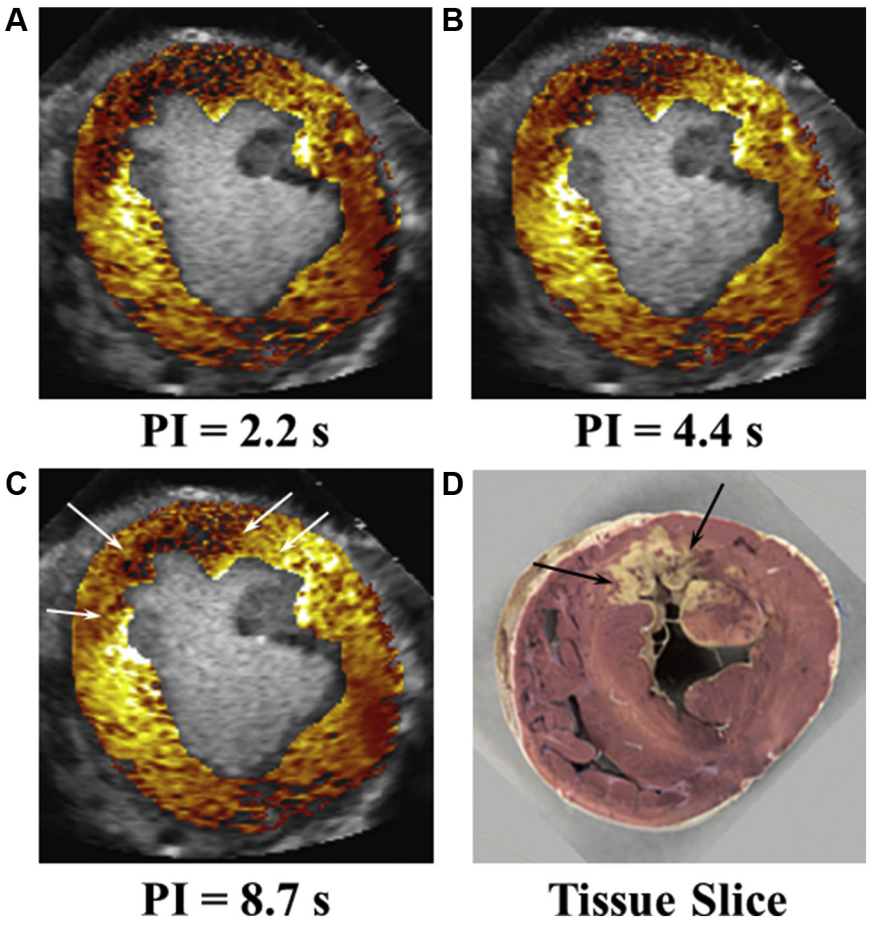

In vivo myocardial contrast echocardiography–defined perfusion defect sizes at various intervals of microbubble replenishment of myocardium and ultimate infarct size on postmortem examination in a dog undergoing 6 hours of coronary occlusion without reperfusion. Although the risk area **(A)** 30 minutes after coronary occlusion appears large, the infarct size is modest **(D)** because of collateral myocardial blood flow **(B and C),** the absence of which clearly defines the spatial extent of necrosis.[93] Thus, even at 30 minutes after coronary occlusion the worst-case scenario infarct size is defined based on myocardial perfusion. **White arrows** define extant of collateral myocardial blood flow laterally. Collateral flow is also present in the epicardium. **Black arrows** define extent of necrosis, which corresponds to area with no perfusion in **C**. PI = pulsing interval.

reperfusion.[93] MCE in this instance was performed during continuous intravenous administration of microbubbles. Using this approach, once steady state is achieved, the microbubbles are destroyed with ultrasound[101] and then images are acquired at increasing pulsing intervals.[102] The risk area defined as region with reduced MBF is illustrated at a short pulsing interval very soon after microbubble replenishment of tissue (Figure 9A), and regions with reduced MBF compared with that of the normal bed are defined at longer pulsing intervals (Figures 9B and 9C).

It is evident that at longer pulsing intervals there is more contrast enhancement in the epicardial and lateral portions of the risk area that represent collateral blood flow. Only regions not receiving collateral blood flow (regions with no contrast enhancement at rest even at long pulsing intervals) at time of coronary occlusion showed infarction 6 hours later. Thus, the MCE image even at the time of coronary occlusion predicted the worst-case scenario infarct size. The transmural migration of necrosis would be arrested with timely reperfusion.

It is interesting to compare the MCE images in Figure 9 with those in Figure 2 where the regions exhibiting reduced MBF reserve after reperfusion also did not include the epicardial and lateral collateralized areas within the risk area. These regions with reduced MBF reserve throughout the

CENTRAL ILLUSTRATION **Mechanism of No Reflow During Acute Myocardial Infarction**

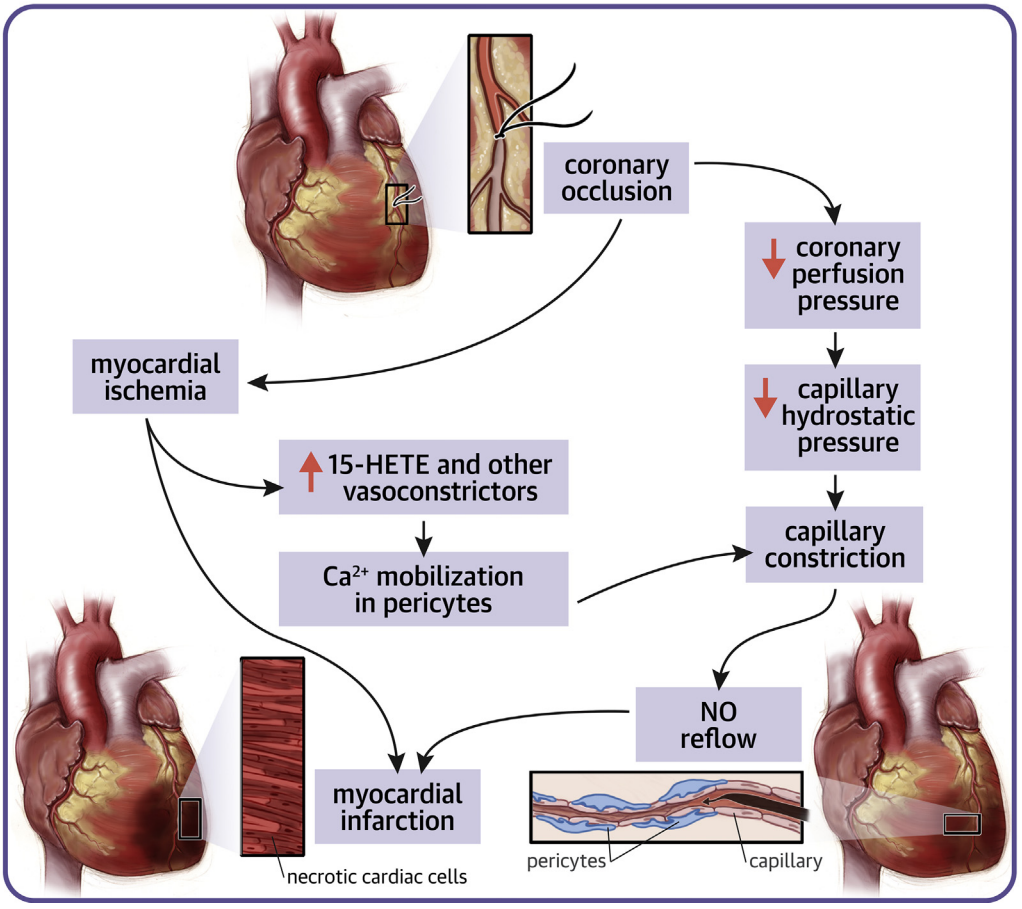

Kaul S, et al. J Am Coll Cardiol Basic Trans Science. 2023;8(2):204–220.

When perfusion pressure drops during coronary occlusion, capillary hydrostatic pressure also drops. In order to keep this pressure constant pericytes contract resulting in capillary constriction and no reflow. Pericytes respond to increased 15-HETE and other vasoconstrictors by mobilizing calcium that results in their contraction. 15-HETE = 15-hydroxyeicosatetraenoic.

duration of reperfusion in Figure 2 later showed necrosis. Could it be that in both instances pericyte contraction caused capillary constriction enough to prevent adequate nutrient blood flow to reach the tissue? Could it also be that the periphery where pericytes (or precapillary sphincters) contracted defined the boundaries of the ultimate infarction? It is expected that if coronary blood flow were to be restored in a timely manner, CHP would rise, pericyte contraction would be reversed, and infarction would be aborted.

Whether pericytes are involved only in no reflow or whether they are also involved in determining the ultimate infarct size has obvious therapeutic implications. The best course of action in a patient presenting with acute myocardial infarction is to attempt reperfusion. However, despite a large reduction in mortality from this approach in the first 2 decades following reperfusion strategies,[103,104] the annual age-adjusted mortality from acute myocardial infarction has remained stubbornly >10% over the past decade.[105] Consequently, newer therapies to improve the outcome in this population would be highly impactful.

SUMMARY

The no-reflow phenomenon has been extensively investigated since 1948 and in the heart since 1966. Although we have learned a great deal about the phenomenon in terms of pathology and potential therapies, there is still a lot to uncover. Pericytes contraction provides a single, cohesive mechanism

underlying the no-reflow phenomenon. It also plays an important role in myocardial ischemia and infarction. Involvement of pericytes in these processes provides an opportunity for use of nonpharmacologic and pharmacologic interventions to relax pericytes and reduce no reflow, infarct size, and degree of ischemia. This could open up new frontiers in the management of acute myocardial infarction (**Central Illustration**).

FUNDING SUPPORT AND AUTHOR DISCLOSURES

Supported by the Garthe and Grace L. Brown Fund of the Oregon Community Foundation. Dr Kaul is one of several inventors mentioned in a provisional patent, filed by Oregon Health and Science University, in the United States for developing drugs to inhibit GPR39;. and he has financial interest in a company (Vasocardea) that has a provisional license from Oregon Health and Science University to commercialize any drugs developed under the patent. A final licensing agreement has not yet been executed. All other authors have reported that they have no relationships relevant to the contents of this paper to disclose.

ADDRESS FOR CORRESPONDENCE: Dr Sanjiv Kaul, Knight Cardiovascular Institute, Oregon Health and Science University, UHN-62, 3181 Southwest Sam Jackson Park Road, Portland, Oregon 97239, USA. E-mail: kauls@ohsu.edu.

REFERENCES

1. Myrdal G, The Challenge of World Poverty. *A World Anti-poverty Program in Outline*. Pantheon Books; 1970.

2. Kloner RA, King KS, Harrington MG. No reflow phenomenon in the heart and brain. *Am J Physiol*. 2018;315(3):H550–H562.

3. Allencherril J, Jneid H, Atar D, et al. Pathophysiology, diagnosis, and management of the no reflow phenomenon. *Cardiovasc Drugs Ther*. 2019;33(5):589–597.

4. Kaul S. The 'no reflow' phenomenon following acute myocardial infarction: mechanisms and treatment options. *J Cardiol*. 2014;64(2):77–85.

5. Majno GA, Ames A, Chaing J, Wright RL. No reflow after cerebral ischemia. *Lancet*. 1967;290:569–570.

6. Harman JW. The significance of local vascular phenomena in the production of ischemic necrosis in skeletal muscle. *Am J Pathol*. 1948;24(3):625–641.

7. Sheehan HL, Davis JC. Renal ischaemia with failed reflow. *J Pathol Bacteriol*. 1959;78:105–120.

8. Kovacs K, Carroll R, Tapp E. Temporary ischaemia of the rat adrenal gland. *J Pathol Bacteriol*. 1966;91(1):235–240.

9. Krug A, de Rochemont WM, Korb G. Blood supply of the myocardium after temporary coronary occlusion. *Circ Res*. 1966;19(1):57–62.

10. Ames A, Wright R, Kowada M, Thurston JM, Majno G. Cerebral ischemia. II. The no-reflow phenomenon. *Am J Pathol*. 1968;52(2):437–453.

11. Kloner RA, Ganote CE, Jennings RB. The "no reflow" phenomenon after temporary coronary occlusion in the dog. *J Clin Invest*. 1974;54(6):1496–1508.

12. Yemisci M, Gursoy-Ozdemir Y, Vural A, Can A, Topalkara K, Dalkara T. Pericyte contraction induced by oxidative-nitrative stress impairs capillary reflow despite successful opening of an occluded cerebral artery. *Nat Med*. 2009;15(9):1031–1037.

13. O'Farrell FM, Mastitskaya S, Hammond-Haley M, Freitas F, Wah WR, Attwell D. Capillary pericytes mediate coronary no reflow after myocardial ischaemia. *Elife*. 2017;6:e29280.

14. Yadava M, Dykan I, Nugent M, et al. Therapeutic ultrasound improves myocardial blood flow and reduces infarct size in a canine model of coronary microthromboembolism. *J Am Soc Echocardiogr*. 2020;33(2):234–246.

15. Sakuma T, Sari I, Goodman NC, Lindner JR, Klibanov A, Kaul S. Simultaneous $\alpha_v\beta_3$ and IIb/IIIa inhibition causes a marked reduction in infarct size following reperfusion in a canine model of acute coronary thrombosis: utility of in-vivo molecular imaging with myocardial contrast echocardiography. *Cardiovasc Res*. 2005;66(3):552–561.

16. Vlaar PJ, Svilaas T, van der Horst IWC, et al. Cardiac death and reinfarction after 1 year in the thrombus aspiration during percutaneous coronary intervention in acute myocardial infarction Study (TAPAS): a 1-year follow-up study. *Lancet*. 2008;371(9628):1915–1920.

17. Burzotta F, Crea F. Thrombus-aspiration: a victory in the war against no reflow. *Lancet*. 2008;371(9628):1889–1890.

18. Kumbhani DJ, Bavry AA, Desai MY, Bangalore S, Bhatt DL. Role of aspiration and mechanical thrombectomy in patients with acute myocardial infarction undergoing primary angioplasty. *J Am Coll Cardiol*. 2013;62(16):1409–1418.

19. Stone GW, Webb J, Cox DA, et al. the Enhanced Myocardial Efficacy and Recovery by Aspiration of Liberated Debris (EMERALD) Investigators. Distal microcirculatory protection during percutaneous coronary intervention in acute ST-segment elevation myocardial infarction: a randomized controlled trial. *JAMA*. 2005;293(9):1063–1072.

20. Ali A, Cox D, Dib N, et al. the AIMI Investigators. Rheolytic thrombectomy with percutaneous coronary intervention for infarct size reduction in acute myocardial infarction: 30-day results from a multicenter randomized study. *J Am Coll Cardiol*. 2006;48(2):244–252.

21. Thiele H, Schindler K, Friedenberger J, et al. Intracoronary compared with intravenous bolus abciximab application in patients with ST-elevation myocardial infarction undergoing primary percutaneous coronary intervention: the randomized Leipzig immediate percutaneous coronary intervention abciximab IV versus IC in ST-elevation myocardial infarction trial. *Circulation*. 2008;118(1):49–57.

22. Danzi G, Sesana M, Capuano C, Mauri L, Centurini PB, Baglini R. Comparison in patients having primary coronary angioplasty of abciximab versus tirofiban on recovery of left ventricular function. *Am J Cardiol*. 2004;94(1):35–39.

23. Heymann MA, Payne BD, Hoffman JI, Rudolph AM. Blood flow measurements with radio-nuclide labeled particles. *Prog Cardiovasc Dis*. 1997;20(1):52–79.

24. Keller MW, Segal SS, Kaul S, Duling BR. The behavior of sonicated albumin microbubbles within the microcirculation: a basis for their use during myocardial contrast echocardiography. *Circ Res*. 1989;65(2):458–467.

25. Jayaweera AR, Edwards N, Glasheen WP, Villanueva FS, Abbott RD, Kaul S. In-vivo myocardial kinetics of air-filled albumin microbubbles during myocardial contrast echocardiography: comparison with radiolabeled red blood cells. *Circ Res*. 1994;74(6):1157–1165.

26. Kaul S. Instrumentation for contrast echocardiography: technology and techniques. *Am J Cardiol*. 2002;90(10A):8J–14J.

27. Kaul S. Myocardial contrast echocardiography: a 25-year retrospective. *Circulation*. 2008;118(3):291–308.

28. Bulluck H, Dharmakumar R, Arai AE, Berry C, Hausenloy DJ. Cardiovascular magnetic resonance in acute ST-segment-elevation myocardial infarction: recent advances, controversies, and future directions. *Circulation*. 2018;137(18):1949–1964.

29. Cobb FR, Bache RJ, Rivas F, Greenfield JC. Local effects of acute cellular injury on regional myocardial blood flow. *J Clin Invest*. 1976;57(5):1359–1368.

30. Willerson JT, Watson JT, Hutton I, Templeton GH, Fixler DE. Reduced myocardial reflow and increased coronary vascular resistance following prolonged myocardial ischemia in the dog. *Circ Res*. 1975;36(6):771–781.

31. Ambrosio G, Weisman HF, Mannisi JA, Becker LC. Progressive impairment of regional myocardial perfusion after initial restoration of

postischemic blood flow. *Circulation*. 1989;80(6):1846–1861.

32. Johnson WB, Malone SA, Pantely GA, Anselone CG, Bristow JD. No reflow and extent of infarction during maximal vasodilation in the porcine heart. *Circulation*. 1988;78(2):462–472.

33. Vanhaecke J, Flameng W, Borgers M, Jang I, Van de Werf F, De Geest H. Evidence for decreased coronary flow reserve in viable post-ischemic myocardium. *Circ Res*. 1990;67(5):1201–1210.

34. Villanueva FS, Glasheen WP, Sklenar J, Kaul S. Characterization of spatial patterns of flow within the re-perfused myocardium using myocardial contrast echocardiography: implications in determining the extent of myocardial salvage. *Circulation*. 1993;88(6):2596–2606.

35. Kaul S, Villanueva FS. Is the determination of myocardial perfusion necessary to evaluate the success of reperfusion when the infarct related artery is open? *Circulation*. 1992;85(5):1942–1954.

36. Villanueva FS, Camarano G, Ismail S, Goodman NC, Sklenar J, Kaul S. Coronary reserve abnormalities during post-infarct reperfusion: implications for the timing of myocardial contrast echocardiography to assess myocardial viability. *Circulation*. 1996;94(4):748–754.

37. Jayaweera AR, Wei K, Coggins M, Bin JP, Goodman C, Kaul S. Role of capillaries in determining coronary blood flow reserve: new insights using myocardial contrast echocardiography. *Am J Physiol*. 1999;277(6):H2363–H2372.

38. Tsagalou EP, Anastasiou-Nana M, Agapitos E. Depressed coronary flow reserve is associated with decreased myocardial capillary density in patients with heart failure due to idiopathic dilated cardiomyopathy. *J Am Coll Cardiol*. 2008;52(17):1391–1398.

39. Kaul S, Jayaweera AR. Myocardial capillaries and coronary flow reserve. *J Am Coll Cardiol*. 2008;52(17):1399–1401.

40. Mohammed SF, Hussain S, Mirzoyef SA, Edwards WD, Maleszewski JJ, Redfield MM. Coronary microvascular rarefaction and myocardial fibrosis in heart failure with preserved ejection fraction. *Circulation*. 2015;131(6):550–559.

41. Methner C, Cao C, Mishra A, Kaul S. Mechanism and potential treatment of the 'no reflow' phenomenon after acute myocardial infarction: role of pericytes and GPR39. *Am J Physiol*. 2021;321(6):H1030–H1041.

42. Methner C, Mishra A, Golgotiu K, et al. Pericyte constriction underlies capillary derecruitment during hyperemia in the setting of arterial stenosis. *Am J Physiol*. 2019;317(2):H255–H263.

43. Ross AM, Gibbons RJ, Stone GW, Kloner RA, Alexander RW. the AMISTAD-II Investigators. A randomized, double-blinded, placebo-controlled multicenter trial of adenosine as an adjunct to reperfusion in the treatment of acute myocardial infarction (AMISTAD-II.). *J Am Coll Cardiol*. 2005;45(11):1775–1780.

44. Marzilli M, Orsini E, Marraccini P, Testa R. Beneficial effects of intracoronary adenosine as an adjunct to primary angioplasty in acute myocardial infarction. *Circulation*. 2000;101(18):2154–2159.

45. Przyklenk K, Kloner RA. "Reperfusion injury" by oxygen-derived free radicals? Effect of superoxide dismutase plus catalase, given at the time of reperfusion, on myocardial infarct size, contractile function, coronary microvasculature, and regional myocardial blood flow. *Circ Res*. 1989;64(1):86–96.

46. Hale SL, Herring MJ, Kloner RA. Delayed treatment with hypothermia protects against the no reflow phenomenon despite failure to reduce infarct size. *J Am Heart Assoc*. 2013;2(1):e004234.

47. Stoel MG, Marques KMJ, de Cock CC, Bronzwaer JGF, von Birgelen C, Zijlstra F. High dose adenosine for suboptimal myocardial reperfusion after primary PCI: a randomized placebo-controlled pilot study. *Catheter Cardiovasc Interv*. 2008;71(3):283–289.

48. Ito H, Taniyama Y, Iwakura K, et al. Intravenous nicorandil can preserve microvascular integrity and myocardial viability in patients with reperfused anterior wall myocardial infarction. *J Am Coll Cardiol*. 1999;33(3):654–660.

49. Ono H, Osanai T, Ishizaka H, et al. Nicorandil improves cardiac function and clinical outcome in patients with acute myocardial infarction undergoing primary percutaneous coronary intervention: role of inhibitory effect on reactive oxygen species formation. *Am Heart J*. 2004;148(4):E15.

50. Taniyama Y, Ito H, Iwakura K, et al. Beneficial effect of intracoronary verapamil on microvascular and myocardial salvage in patients with acute myocardial infarction. *J Am Coll Cardiol*. 1997;30(5):1193–1199.

51. Huang D, Qian JY, Ge L, et al. Effects of different routes of intracoronary infusion of verapamil on no reflow phenomenon during percutaneous coronary intervention in patients with acute myocardial infarction. *Eur Heart J*. 2013;34(suppl 1):eht309. P3974.

52. Headrick JP, Lasley RD. Adenosine receptors and reperfusion injury of the heart. *Handb Exp Pharmacol*. 2009;193:189–214.

53. Zheng Y, Li X, Zhang F, et al. Protective effect of nicorandil against myocardial ischemia/reperfusion injury mediated via IL33/ST2 signaling pathway. *Mol Cell Biochem*. 2022;477(7):1921–1929.

54. Coetzee A, Conradie S. Calcium antagonist verapamil and reperfusion injury of the heart. *J Cardiothor Vasc Anesth*. 2007;21(3):337–343.

55. Tsamatsoulis M, Kapelios CJ, Katsaros L, et al. Cardioprotective effects of intracoronary administration of 4-chlorodiazepam in small and large animal models of ischemia-reperfusion. *Int J Cardiol*. 2016;224:90–95.

56. Han X, Wu Y, Liu X, et al. Adiponectin improves coronary no reflow injury by protecting the endothelium in rats with type 2 diabetes mellitus. *Biosci Rep*. 2017;37(4):BSR20170282.

57. Ichimura K, Matoba T, Nakano K, et al. A translational study of a new therapeutic approach for acute myocardial infarction: nanoparticle-mediated delivery of pitavastatin into reperfused myocardium reduces ischemia-reperfusion injury in a preclinical porcine model. *PLoS One*. 2016;11(9):e0162425.

58. Song K, Wang Y, Sheng J, Ma C, Li H. Effects of dabigatran regulates no-reflow phenomenon in acute myocardial infarction mice through anti-inflammatory and anti-oxidative activities and connective tissue growth factor expression. *Mol Med Report*. 2018;17(1):580–585.

59. Hernandez-Resendiz S, Palma-Flores C, De Los Santos S, et al. Reduction of no-reflow and reperfusion injury with the synthetic 17beta-aminoestrogen compound Prolame is associated with PI3K/Akt/eNOS signaling cascade. *Basic Res Cardiol*. 2015;110(2):1.

60. Hale SL, Kloner RA. The antianginal agent, ranolazine, reduces myocardial infarct size but does not alter anatomic no reflow or regional myocardial blood flow in ischemia/reperfusion in the rabbit. *J Cardiovasc Pharmacol Ther*. 2008;13(3):226–232.

61. Dai W, Cheung E, Alleman RJ, et al. Cardioprotective effects of mitochondria-targeted peptide SBT-20 in two different models of rat ischemia/reperfusion. *Cardiovasc Drugs. Ther*. 2016;30(6):559–566.

62. Skyschally A, Amanakis G, Neuhauser M, Kleinbongard P, Heusch G. Impact of electrical defibrillation on infarct size and no reflow in pigs subjected to myocardial ischemia-reperfusion without and with ischemic conditioning. *Am J Physiol*. 2017;313(5):H871–H878.

63. Le ED, Davis C, Wei K, et al. Ranolazine exhibits its beneficial properties by increasing myocardial adenosine levels. *Am J Physiol*. 2020;318(1):H189–H202.

64. Lasley RD, Jahania MS, Mentzer RM Jr. Beneficial effects of adenosine A(2a) agonist CGS-21680 in infarcted and stunned porcine myocardium. *Am J Physiol*. 2001;280(4):H1660–H1666.

65. Le DE, Jayaweera AR, Wei K, Coggins MP, Lindner JR, Kaul S. Changes in myocardial blood volume over a wide range of coronary driving pressures: role of capillaries beyond the autoregulatory range. *Heart*. 2004;90(10):1199–1205.

66. Kaul S, Methner C, Mishra A. The role of pericytes in hyperemia-induced capillary derecruitment following stenosis. *Curr Tissue Microenviron Rep*. 2020;1(4):163–169.

67. Starling EH. On the absorption of fluids from the connective tissue spaces. *J Physiol*. 1896;19(4):312–326.

68. Martini J, Honig CR. Direct measurement of intercapillary distance in beating rat heart in situ under various conditions of O 2 supply. *Microvasc Res*. 1969;1(3):244–256.

69. Grubb S, Cai C, Hald BO, et al. Precapillary sphincters maintain perfusion in the cerebral cortex. *Nat Commun*. 2020;11(1):395.

70. Nakano M, Atobe Y, Goris RC, et al. Ultrastructure of the capillary pericytes and the expression of smooth muscle alpha-actin and desmin the snake infrared sensory organs. *Anat Rec*. 2000;260(3):299–307.

71. Higuchi K, Hashizume H, Aizawa Y, Ushiki T. Scanning electron microscopic studies of the vascular smooth muscle cells and pericytes in the rat heart. *Arch Histol Cytol*. 2000;63(2):115–126.

72. Nees S, Weiss DR, Juchem G. Focus on cardiac pericytes. *Pflugers Arch*. 2013;465(6):779–787.

73. Rouget C. Note sur le développement de la tunique contractile des vaisseaux. *Compt Rend Acad Sci*. 1874;59:559–562.

74. Hartmann DA, Underly RG, Grant RI, Watson AN, Lindner V, Shih AY. Pericyte structure and distribution in the cerebral cortex revealed by high-resolution imaging of transgenic mice. *Neurophotonics*. 2015;2(4):041402.

75. Biesecker KR, Srienc AI, Shimoda AM, et al. Glial cell calcium signaling mediates capillary regulation of blood flow in the retina. *J Neurosci*. 2016;36(36):9435–9445.

76. Mishra A, Reynolds JP, Chen Y, Gourine AV, Rusakov DA, Attwell D. Astrocytes mediate neurovascular signaling to capillary pericytes but not to arterioles. *Nat Neurosci*. 2016;106(12):1619–1627, 19.

77. Hall CN, Reynell C, Gesslein B, et al. Capillary pericytes regulate cerebral blood flow in health and disease. *Nature*. 2014;508(7494):55–60.

78. Alex L, Frangogiannis NG. Pericytes in the infarcted heart. *Vasc Biol*. 2019;1(1):H23–H31.

79. Das A, Frank RN, Weber ML, Kennedy A, Reidy CA, Mancini MA. ATP causes retinal pericytes to contract in vitro. *Exp Eye Res*. 1988;46(3):349–362.

80. Kelley C, D'Amore P, Hechtman HB, Shepro D. Microvascular pericyte contractility in vitro: comparison with other cells of the vascular wall. *J Cell Biol*. 1987;104(3):483–490.

81. Lee S, Zeiger A, Maloney JM, Kotecki M, Van Vliet KJ, Herman IM. Pericyte actomyosin-mediated contraction at the cell-material interface can modulate the microvascular niche. *J Phys Condens Matter*. 2010;22(19):194115.

82. Le DE, Zhao Y, Kaul S. Persistent coronary vasomotor tone during myocardial ischemia occurs at the capillary level and may involve pericytes. *Front Cardiovasc Med*. 2022;9:930492. https://doi.org/10.3889/fcvm.2022.930492

83. Castellano G, Franzin R, Stasi A, et al. Complement activation during ischemia/reperfusion injury induces pericyte-to-myofibroblast transdifferentiation regulating peritubular capillary lumen reduction through pERK signaling. *Front Immunol*. 2018;9:01002.

84. Heyba M, Al-Abdullah L, Henkel AW, Sayed Z, Malatiali SA, Redzic ZB. Viability and contractility of rat brain pericytes in conditions that mimic stroke; an in vitro study. *Front Neurosci*. 2019;13:1306.

85. Alarcon-Martinez L, Yilmaz-Ozcan S, Yemisci M, Schallek J, et al. Retinal ischemia induces α-SMA-mediated capillary pericyte contraction coincident with perivascular glycogen depletion. *Acta Neuropathol Commun*. 2019;7(1):134.

86. Hariharan A, Weir N, Robertson C, He L, Betsholtz C, Longden TA. The ion channel and GPCR toolkit of brain capillary pericytes. 2020. *Front Cell Neurosci*. 2020;14:601324. Accessed April 15, 2021. https://www.frontiersin.org/article/10.3389/fncel.2020.601324

87. Matsugi T, Chen Q, Anderson DR. Adenosine-induced relaxation of cultured bovine retinal pericytes. *Invest Ophthalmol Vis Sci*. 1997;38(13):2695–2701.

88. Li Q, Puro DG. Adenosine activates ATP-sensitive K(+) currents in pericytes of rat retinal microvessels: role of A1 and A2a receptors. *Brain Res*. 2001;907(1-2):93–99.

89. Nakae I, Matsumoto T, Horie H, et al. Effects of intravenous nicorandil on coronary circulation in humans: plasma concentration and action mechanism. *J Cardiovasc Pharmacol*. 2000;35(6):919–925.

90. Gonzales AL, Klug NR, Moshkforoush A, et al. Contractile pericytes determine the direction of blood flow at capillary junctions. *Proc Natl Acad Sci U S A*. 2020;117(43):27022–27033.

91. Alkayed NJ, Cao Z, Qian ZY, et al. Control of coronary vascular resistance by eicosanoids via a novel GPCR. *Am J Physiol Cell Physiol*. 2022;322(5):C1011–C1021.

92. Reimer KA, Lowe JE, Rasmussen MM, Jennings RB. The wavefront phenomenon of ischemic cell death. 1. Myocardial infarct size vs duration of coronary occlusion in dogs. *Circulation*. 1977;56(5):786–794.

93. Coggins MP, Le DE, Wei K, Goodman NC, Lindner JR, Kaul S. Noninvasive prediction of ultimate infarct size at the time of acute coronary occlusion based on the extent and magnitude of collateral-derived myocardial blood flow. *Circulation*. 2001;104(20):2471–2477.

94. Müller KD, Sass S, Gottwik MG, Schaper W. Effect of myocardial oxygen consumption on infarct size in experimental coronary artery occlusion. *Basic Res Cardiol*. 1982;77(2):170–181.

95. Gerdes AM, Callas G, Kasten FH. Differences in regional capillary distribution and myocyte sizes in normal and hypertrophic rat hearts. *Am J Anat*. 1979;156(4):523–531.

96. Stoker ME, Gerdes AM, May JF. Regional differences in capillary density and myocyte size in the normal human heart. *Anat Rec*. 1982;202(2):187–191.

97. Canty JM Jr, Klocke FJ. Reduced regional myocardial perfusion in the presence of pharmacologic vasodilator reserve. *Circulation*. 1985;71(2):370–377.

98. Aversano T, Becker LC. Persistence of coronary vasodilator reserve despite functionally significant flow reduction. *Am J Physiol*. 1985;248(3 Pt 2):H403–H411.

99. Pantely GA, Bristow JD, Swenson LJ, Ladley HD, Johnson WB, Anselone CG. Incomplete coronary vasodilation during myocardial ischemia in swine. *Am J Physiol*. 1985;249(3 Pt 2):H638–H647.

100. Lindner JR, Skyba DM, Goodman NC, Jayaweera AR, Kaul S. Changes in myocardial blood volume with graded coronary stenosis: an experimental evaluation using myocardial contrast echocardiography. *Am J Physiol*. 1997;272(1 Pt 2):H567–H57.

101. Wei K, Skyba DM, Firschke C, Lindner JR, Jayaweera AR, Kaul S. Interaction between microbubbles and ultrasound: in vitro and in vivo observations. *J Am Coll Cardiol*. 1997;29(5):1081–1088.

102. Wei K, Firoozan S, Jayaweera AR, Linka A, Skyba D, Kaul S. Quantification of myocardial blood flow with ultrasound-induced destruction of microbubbles administered as a continuous infusion. *Circulation*. 1998;97(5):473–482.

103. Ford ES, Ajani UA, Croft JB, et al. Explaining the decrease in U.S. deaths from coronary disease, 1980-2000. *N Engl J Med*. 2007;356(23):2388–2398.

104. Krumholz HM, Wang Y, Chen J, et al. Reduction in acute myocardial infarction mortality in the United States: risk-standardized mortality rates from 1995-2006. *JAMA*. 2009;302(7):767–773.

105. Dani SS, Lone AN, Javed Z, et al. Trends in premature mortality from acute myocardial infarction in the united states, 1999 to 2019. *J Am Heart Assoc*. 2022;11(1):e021682.

KEY WORDS acute myocardial infarction, blood flow, necrosis, no reflow, pericytes